

Preparation, magnetoresistance and magnetocaloric effect of two-layered perovskite $\text{La}_{2.5-x}\text{K}_{0.5+x}\text{Mn}_2\text{O}_{7+\delta}$

W. Zhong^{1,a}, W. Chen², H.Y. Jiang¹, X.S. Liu¹, C.T. Au³, and Y.W. Du¹

¹ National Laboratory of Solid State Microstructures, Nanjing University, Nanjing 210093, PR China

² Department of Physics, Hebei Normal University, Shijiazhuang 050091, PR China

³ Chemistry Department and Center for Surface Analysis and Research, Hong Kong Baptist University, Kowloon Tong, PR China

Received 2 May 2002 / Received in final form 1st October 2002

Published online 19 December 2002 – © EDP Sciences, Società Italiana di Fisica, Springer-Verlag 2002

Abstract. Polycrystalline two-layered perovskite $\text{La}_{2.5-x}\text{K}_{0.5+x}\text{Mn}_2\text{O}_{7+\delta}$ ($0 < x < 0.5$) samples have been prepared by a modified sol-gel method and their magnetoresistance and magnetocaloric effects have been studied. A large deviation between the metal-insulator (MI) transition temperature (T_ρ) and the magnetic transition temperature (T_C) is observed. Large magnetoresistance (MR) effects with $\Delta\rho/\rho_0$ of $\sim 40\%$ at 12 kOe are obtained in wide temperature ranges. The maximum of the magnetic entropy change peaks at its Curie temperature (T_C), far above its MI transition temperature (T_ρ). The large magnetic entropy change (~ 1.4 J/kg.K) is obtained in the sample $\text{La}_{2.5-x}\text{K}_{0.5+x}\text{Mn}_2\text{O}_{7+\delta}$ ($x = 0.35$) upon 10 kOe applied magnetic field.

PACS. 75.30.Sg Magnetocaloric effect, magnetic cooling – 82.80.-d Chemical analysis and related physical methods of analysis – 81.05.Mh Cermets, ceramic and refractory composites

1 Introduction

The discovery of the colossal magnetoresistance (CMR) [1–7] and large magnetocaloric (MC) [8–12] effects in mixed-valence manganese perovskites has attracted great attention with regard to scientific investigation and technological applications. So far, most of the research work on the magnetic and transport properties of manganese compounds has been devoted to ABO_3 -type lanthanide manganese perovskites $\text{Ln}_{1-x}\text{A}_x\text{MnO}_3$ ($\text{Ln} = \text{La, Pr, Nd, Sm}$; $\text{A} = \text{Ca, Sr, Ba or Pb}$). Recently, much attention in those fields has been focused on the layered variants of the perovskite $\text{A}_{n+1}\text{B}_n\text{O}_{3n+1}$. Apart from ABO_3 -type ($n = \infty$) manganates with three-dimensional Mn-O networks, $\text{A}_{n+1}\text{B}_n\text{O}_{3n+1}$ -type compounds gave rise to a special interest due to their crystal structure forming a natural layered tunneling system. Investigation results [13–23] have indicated that the reduced dimensionality of the Mn-O-Mn networks leads to several intriguing changes in features of the ferromagnetic manganate perovskites, including enhanced magnetoresistance effects, large magnetocaloric effects, unconventional magnetostriiction and anisotropic transport in charge carriers. Moreover, these layered systems exhibit a variety of both ferromagnetic and antiferromagnetic structures, such as paramagnetic insulating (PI) state, antiferromagnetic

metallic (AFM), ferromagnetic metallic (FM), canted antiferromagnetic (CAF), antiferromagnetic insulating (AFI), and charge-ordered (CO) states, etc. [24–31].

It is known that the investigations of two-layered perovskites are focused on alkaline-earth (such as Ca and Sr)-doped lanthanide manganites, but to the best of our knowledge, references to magnetic and electronic properties of monovalent alkali-metal-doped layered-perovskites are very scarce. By taking into consideration that the donor property of alkali-metal is stronger than that of alkaline-earth-metal, it would be expected that alkali-metal-doped two-layered perovskite manganites exhibit distinguishing features in structure, electronic behavior, and magnetic properties from the alkaline-earth-doped lanthanide manganites. In the present work, we have synthesized the polycrystalline two-layered perovskite $\text{La}_{2.5-x}\text{K}_{0.5+x}\text{Mn}_2\text{O}_{7+\delta}$ ($0 < x < 0.5$) by a modified sol-gel method, and investigated their structures, the magnetoresistance and magnetocaloric effects.

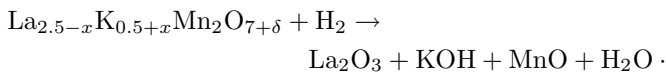
2 Experimental

The polycrystalline two-layered perovskite $\text{La}_{2.5-x}\text{K}_{0.5+x}\text{Mn}_2\text{O}_{7+\delta}$ ($x = 0.05, 0.15, 0.25, 0.35$ and 0.45) samples were prepared by a modified sol-gel method as follows [32]: Stoichiometric amounts of La_2O_3 (99.99%), K_2CO_3 , and $\text{Mn}(\text{NO}_3)_2$ were dissolved in dilute

^a e-mail: wzhong@ufp.nju.edu.cn

HNO₃ solution at 333 K. Then suitable amounts of citric acid and ethylene glycol were added as coordinate agents to generate a completely homogeneous and transparent solution. This solution was subjected to slow evaporation at 333 K until a highly viscous residual was formed. With further heating at 443 K, a gel was developed. The gel was thermally treated at 873 K for 5 hours to decompose the organic precursor. After being ground, the samples were calcined in air at 1173 K and furnace cooled. The calcined materials were pressed into round disks, and a final sintering process step was carried out at 1173 K for 5 h, 1473 K for 2h and furnace cooled.

Phase identification and structural analysis were examined by X-ray powder diffraction with Cu K α radiation (Model D/Max-RA, Rigaku, Japan). The metal content in the sintered sample was determined by induced coupled plasma (ICP) spectroscopy (Model 1100 + 2000, Jarrell-Ash, USA). The oxygen content in these La_{2.5-x}K_{0.5+x}Mn₂O_{7+ δ} samples was determined by a temperature-programmed reduction (TPR) technique [33,34]. In our present experiment, Ar + H₂ (15.0% V/V) mixed gas flushed over the sample, which was heated at a linear rate (6 K/min), and the concentration of H₂ in the mixed gas was monitored simultaneously by a thermal conductivity detector (TCD). The oxygen content in the sample was deduced from the consumption of H₂ in reaction between H₂ and the sample, based on the following equation (the valences of lanthanum and alkali-metal were conserved, while the Mn³⁺, Mn⁴⁺ were reduced to Mn²⁺ in the reaction):



The morphology of La_{2.5-x}K_{0.5+x}Mn₂O_{7+ δ} ($0 < x < 0.5$) was examined directly by transmission electron microscopy (TEM) (Model JEM-200 CX, JEOL, Japan) and their average crystallite size was estimated by means of XRD line broadening analysis. M - T and M - H curves were measured by a vibrating sample magnetometer (VSM) (Model PAR 155, USA). Curie temperature (T_C) was determined from the M - T curves. Magnetization of the samples was measured in an isothermal regime under an applied magnetic field varying from 0 to 10 kOe. In the vicinity of T_C , isothermal M - H curves were obtained by a step of 3 or 5 K. The electrical resistance and magnetoresistance of these samples were measured as a function of temperature (80–300 K) and magnetic field (0–12 kOe) by the standard four-probe technique. Electrical contacts were made with silver paste.

3 Results and discussion

3.1 Structure and composition

The grain sizes of La_{2.5-x}K_{0.5+x}Mn₂O_{7+ δ} samples (calcined at 1473 K) observed directly by TEM images are 550 to 750 nm. Their average crystallite sizes determined

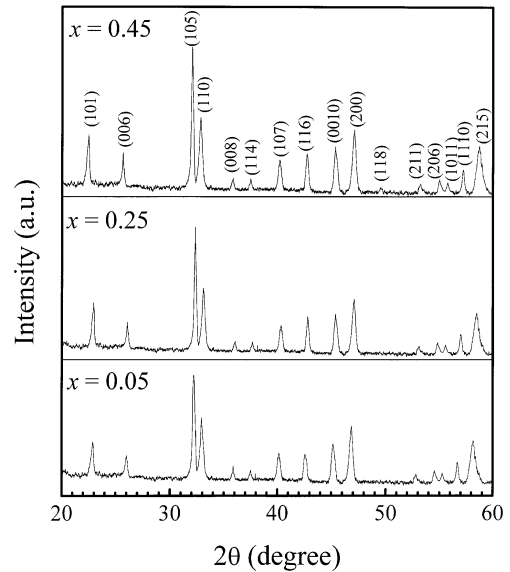


Fig. 1. X-ray diffraction pattern of La_{2.5-x}K_{0.5+x}Mn₂O_{7+ δ} samples.

by XRD are 90 to 165 nm, significantly smaller than the values determined by TEM. A particle may exist as a single unit, *e.g.* a single crystal, or it may consist of subunits. The small subunits are defined as the primary particles and the agglomerates of these primary particles are called secondary particles. Observations by imaging techniques such as TEM often give the size of the secondary particles, and the X-ray line broadening analysis disclosed the size of primary particles. The X-ray diffraction patterns for polycrystalline samples of La_{2.5-x}K_{0.5+x}Mn₂O_{7+ δ} are shown in Figure 1. For all the studied compositions, $0 < x < 0.5$, La_{2.5-x}K_{0.5+x}Mn₂O_{7+ δ} materials have the tetragonal Sr₃Ti₂O₇-type perovskite structure (I4/mmm). As x increase, the measured lattice parameters at room temperature increase monotonically from $a = 3.8574$ Å and $c = 20.1688$ Å ($x = 0.05$) to $a = 3.8745$ Å and $c = 20.3379$ Å ($x = 0.45$), respectively. It is important to mention that XRD technique cannot detect impurity phase less than 3 to 5%. According as our present experimental results, we cannot obviate the possibility of the presence of a small quantity of other phases in our polycrystalline samples. It is well known that normally a sample with nominal $n = 2$ phase contains intergrowths and the presence of other phases such as $n > 2$ is rather difficult to avoid. So, further exploration of the phase identification and structural analysis of these samples may be needed.

Table 1 summarizes the results of the ICP and TPR measurements. As can be seen, the actual alkali-metal content for all the compositions explored in this work is practically close to the nominal one. The average manganese oxidation state $\langle V_{\text{Mn}} \rangle$ calculated from electric neutrality is also listed in Table 1. One can observe that $\langle V_{\text{Mn}} \rangle$ tends to increase when the K content x increases.

Figure 2 shows schematic view of layer sequences of ABO₃-type ($n = \infty$) and A₃B₂O₇-type ($n = 2$)

Table 1. Summary of the results of ICP and TPR measurements, and physical properties of $\text{La}_{2.5-x}\text{K}_{0.5+x}\text{Mn}_2\text{O}_{7+\delta}$ samples. $\langle V_{\text{Mn}} \rangle$, T_C and T_ρ mean the average manganese oxidation state, Curie temperature, and the peak temperature in resistivity, respectively.

X^a	La/Mn	K/Mn	δ	$\langle V_{\text{Mn}} \rangle$	T_C	T_ρ	Stoichiometry
0.05	1.231	0.262	0.06	3.11	200	—	$\text{La}_{2.441}\text{K}_{0.519}\text{Mn}_{1.983}\text{O}_7$
0.15	1.170	0.305	0.07	3.26	225	115	$\text{La}_{2.317}\text{K}_{0.604}\text{Mn}_{1.980}\text{O}_7$
0.25	1.120	0.340	0.03	3.33	235	128	$\text{La}_{2.230}\text{K}_{0.677}\text{Mn}_{1.991}\text{O}_7$
0.35	1.073	0.391	0.03	3.42	247	153	$\text{La}_{2.137}\text{K}_{0.779}\text{Mn}_{1.991}\text{O}_7$
0.45	1.032	0.468	0.01	3.45	254	165	$\text{La}_{2.061}\text{K}_{0.935}\text{Mn}_{1.997}\text{O}_7$

^a Nominal composition.

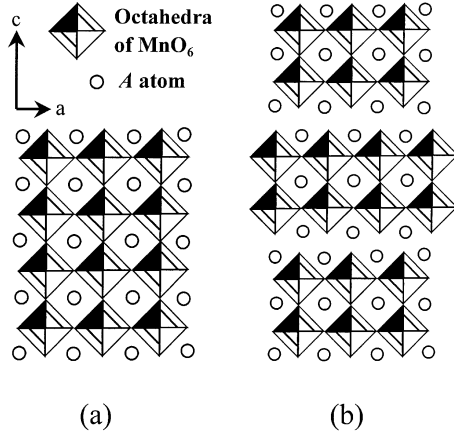


Fig. 2. Schematic view of layer sequences of (a) ABO_3 -type ($n = \infty$) and (b) $\text{A}_3\text{B}_2\text{O}_7$ -type ($n = 2$) perovskite compounds.

perovskite compounds [14]. The ABO_3 -type manganese compound consists of perovskite units with three-dimensional Mn-O networks. In contrast, the $\text{A}_3\text{B}_2\text{O}_7$ -type two-layered manganite exhibits two-dimensional Mn-O networks and contains double perovskite layers interleaved with A-O layers. In the $\text{La}_{2.5-x}\text{K}_{0.5+x}\text{Mn}_2\text{O}_{7+\delta}$ system, double perovskite layers are interleaved with La(K)O layers, and Mn-O-Mn bonds in the c -axis direction are separated from one another by La(K)O layers. Among the structural consequence of moving from ABO_3 -type perovskite to $\text{A}_3\text{B}_2\text{O}_7$ -type manganite are the introduction of a two-dimensional character and a reduction from 6 to 5 in the number of nearest-neighbor Mn cations around each transition-metal site. This is expected to produce an anisotropic reduction in the width of the energy bands derived from the Mn $3d$ orbitals, and hence to modify the electrical and magnetic properties.

3.2 Magnetic and electrical properties

The ferromagnetic ordering transition temperature, T_C , defined as the temperature at which the $dM/dT \sim T$ curve reaches a minimum, has been extracted from the low field magnetization (1 kOe) *versus* temperature. As x increases, the T_C values increase from 200 K ($x = 0.05$) and 235 K ($x = 0.25$) to 253 K ($x = 0.45$) (see Tab. 1).

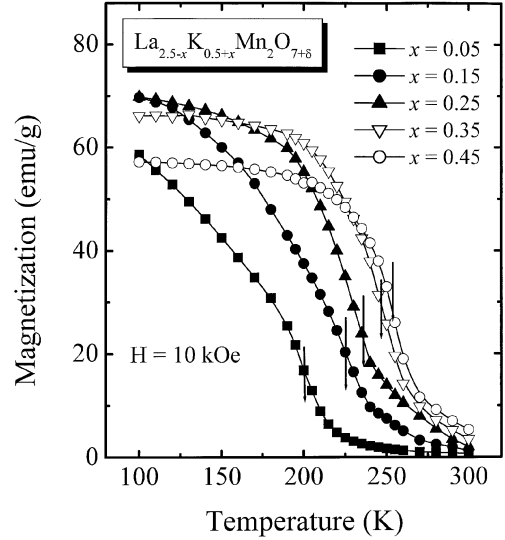


Fig. 3. Temperature dependence of zero-field cooled (ZFC) magnetization (warming curves) for polycrystalline $\text{La}_{2.5-x}\text{K}_{0.5+x}\text{Mn}_2\text{O}_{7+\delta}$ samples. The Curie temperature (T_C) is marked with an arrow.

Figure 3 displays the temperature dependence of the magnetization (M) for samples $\text{La}_{2.5-x}\text{K}_{0.5+x}\text{Mn}_2\text{O}_{7+\delta}$. The magnetization was measured upon warming in a field of 10 kOe after cooling to 100 K in zero field. As x increases from $x = 0.05$, the M at 100 K first increases from 58.6 emu/g ($3.06 \mu_B/\text{Mn}$, $x = 0.05$) to 69.8 emu/g ($3.50 \mu_B/\text{Mn}$, $x = 0.25$), and then decreases to 57.2 emu/g ($2.80 \mu_B/\text{Mn}$, $x = 0.45$). The M value of $3.50 \mu_B/\text{Mn}$ ($x = 0.25$) is in good agreement with the expected value of $3.67 \mu_B/\text{Mn}$ for the average oxidation state of 3.33 for Mn cations, indicating that the $x = 0.25$ sample possesses a good ordered spin alignment. A reduced magnetic moment in the lower x range may suggest a canted ferromagnetic spin arrangement. The large reduction in the magnetic moment in the higher x range could be ascribed to the contribution of the antiferromagnetic interaction between Mn^{4+} cations. In Figure 4, we show the temperature dependence of the resistivity ρ for the polycrystalline $\text{La}_{2.5-x}\text{K}_{0.5+x}\text{Mn}_2\text{O}_{7+\delta}$ series ($0 < x < 0.5$). For $x = 0.05$, the ρ - T curve is characteristic of semiconductor or insulator. For $x \geq 0.15$, the ρ - T curve exhibits a peak (Hereafter, the peak temperature in resistivity is designated as T_ρ). With increments in the K content x from 0.25 up to 0.45, T_ρ increased from 128 K to 165 K and the

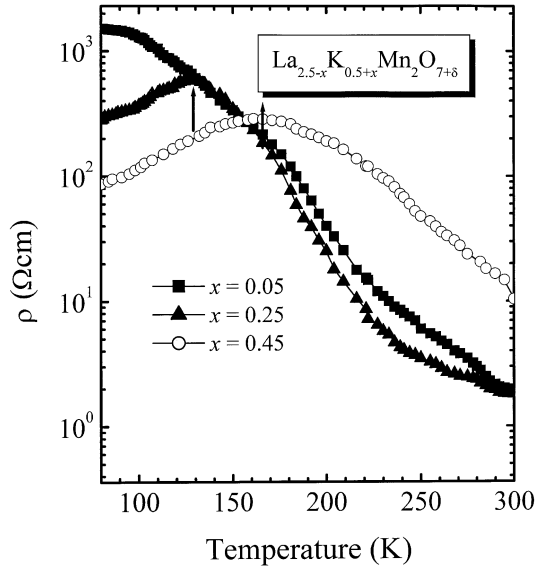


Fig. 4. Temperature dependence of the resistivity ρ for the sample $\text{La}_{2.5-x}\text{K}_{0.5+x}\text{Mn}_2\text{O}_{7+\delta}$. The peak temperature in resistivity (T_ρ) is marked with an arrow.

resistivity decreased. When comparing the T_ρ values with the T_C values for corresponding doping concentrations, the T_ρ values were about 100 K lower than the T_C values. In other words, for the $\text{La}_{2.5-x}\text{K}_{0.5+x}\text{Mn}_2\text{O}_{7+\delta}$ polycrystalline series, a large deviation between the metal-insulator transition and the magnetic transition is observed. This phenomenon could be ascribed to three factors: the special structure of layered-perovskite, the grain boundary effect and the influence of impurity.

We now consider the structural relationship between $\text{La}_{2.5-x}\text{K}_{0.5+x}\text{Mn}_2\text{O}_{7+\delta}$ and ABO_3 -type perovskite. As a consequence of the structural change from ABO_3 -type perovskite down to its two-layered variants, $\text{La}_{2.5-x}\text{K}_{0.5+x}\text{Mn}_2\text{O}_{7+\delta}$, which is brought about by insertion of the insulating $(\text{La}, \text{K})\text{O}_2$ into the perovskite MnO_2 bilayers (hereafter MnO_2 bilayers were denoted as a - b plane and perpendicular to this plane as c direction), a two-dimensional character is introduced. This is expected to produce anisotropic exchange interactions, namely: the intralayer exchange interaction, which works within a perovskite MnO_2 bilayers, and interlayer exchange interaction, which acts between perovskite MnO_2 bilayers. The former is due to the double-exchange interaction, and is perhaps much stronger than the latter. Asano and co-workers [35] reported systematic results on the resistivity and magnetization of layered perovskite $\text{La}_{2-2x}\text{Ca}_{1+2x}\text{Mn}_2\text{O}_7$ ($0 \leq x \leq 0.5$) and observed that these layered manganites exhibited a metal-insulator transition temperature (T_ρ) far (100 K) below the magnetic transition temperature T_C . They assume that the layered perovskite $\text{La}_{2-2x}\text{Ca}_{1+2x}\text{Mn}_2\text{O}_7$ exhibits two types of ferromagnetic ordering caused by the anisotropic carrier transport and exchange interaction. The electrical properties of the bulk samples are dominated by less conductive transport along the c di-

rection, which is due to a weaker exchange interaction. By contrast, the magnetic transitions of the bulk materials are governed by the strong in-plane exchange interaction. Thus, T_ρ is observed far below the T_C of the bulk samples. We observed similar phenomena for the polycrystalline samples of $\text{La}_{2.5-x}\text{K}_{0.5+x}\text{Mn}_2\text{O}_{7+\delta}$, and would be partly due to the same mechanism. However, a good correlation was observed between T_ρ and T_C for the layered perovskite $\text{La}_{2-2x}\text{Sr}_{1+2x}\text{Mn}_2\text{O}_7$ [13]. Therefore other factors could also be considered. It is important to mention that an extrinsic effect, such as grain size, would also result in a large deviation in T_ρ and T_C . Mahendiran *et al.* [36,37] found that for bulk samples of cubic perovskite with a small grain size less than $0.5 \mu\text{m}$, their metal-insulator transition temperatures (T_ρ) are significantly lower (~ 170 K) than the corresponding Curie temperatures. They suggested that as the grain size decreases, the relative contribution of the insulating region increase making ρ large and lowering T_ρ . Another possible reason for the deviation between T_ρ and T_C could be the presence of a small quantity of impurity such as $n > 2$ phases which may not be detected by XRD. When K doping level x ranged between 0.075 and 0.20, the ABO_3 -type polycrystalline $\text{La}_{1-x}\text{K}_x\text{MnO}_{3+\delta}$ samples exhibit paramagnetic-to-ferromagnetic phase transitions at 230–344 K [32], higher than that of corresponding layered manganites. This means that a reduction in the dimensionality from $n = \infty$ to $n = 2$ should result in a reduction in T_C .

3.3 Magnetoresistance effect

The temperature dependence of the MR ratio of $\text{La}_{2.5-x}\text{K}_{0.5+x}\text{Mn}_2\text{O}_{7+\delta}$ samples for the concentrations of $x = 0.05, 0.15, 0.25, 0.35,$ and 0.45 is shown in Figure 5. The MR ratio here is defined as $-\Delta\rho/\rho_0 = -(\rho_H - \rho_0)/\rho_0$ (where ρ_H and ρ_0 are the resistivity in an applied magnetic field and the zero field resistivity, respectively). It can be seen that the MR effect of these samples exhibits a complicated temperature dependence over a wide temperature range. The MR at $H = 12$ kOe does not show a clear peak and there is a systematic increase with decreasing temperatures in all samples. This MR behavior is quite different from that of the ABO_3 -type perovskite manganites. It is well known that in conventional perovskites such as $\text{La}_{1-x}(\text{Ca}, \text{Sr})_x\text{MnO}_3$, CMR effects are restricted to a narrow temperature range where a ferromagnetic metal to paramagnetic insulator transition takes place. The large MR effect ($-\Delta\rho/\rho_0 \sim 40\%$) is obtained in the sample $\text{La}_{2.5-x}\text{K}_{0.5+x}\text{Mn}_2\text{O}_{7+\delta}$ ($x = 0.35$) with 12 kOe magnetic field.

The most notable feature in the two-layered perovskite manganite is the behavior in the $T < T_C$ range, where the MR effects are quite large under a relatively lower magnetic field. The origin of the enhanced low-field MR effects in this compound could be ascribed to anisotropic Mn-O networks with reduced dimensions. The simple explanation would be that the two dimensionality of the Mn-O

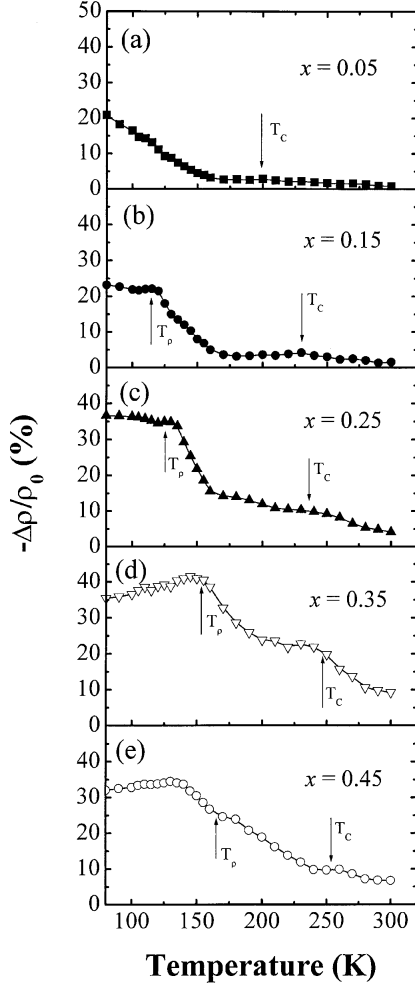


Fig. 5. Temperature dependence of magnetoresistance under an applied field of 12 kOe for samples $\text{La}_{2.5-x}\text{K}_{0.5+x}\text{Mn}_2\text{O}_{7+\delta}$. (a) $x = 0.05$, (b) $x = 0.15$, (c) $x = 0.25$, (d) $x = 0.35$, and (e) $x = 0.45$.

networks causes a reduction in the effective transfer interaction of the e_g carriers, which gives rise to enhanced effective coupling between the local spin and the charge carrier *via* strong intra-atomic ferromagnetic (Hund) coupling. An additional and more important factor is the anisotropic exchange interaction in this compound. The intra-layer exchange interaction is obviously due to the double-exchange interaction, and is perhaps much stronger than the inter-layer value. An external magnetic field could easily restore the two-dimensional spin order and therefore enhance the transfer of the conduction electrons, thus giving rise to large MR effects with a relatively lower magnetic field in this temperature range.

3.4 Magnetocaloric properties

The entropy change, which results from the spin ordering (*i.e.*, ferromagnetic ordering) and is induced by the

variation of the applied field from 0 to H_{\max} , is given by

$$|\Delta S_M| = \int_0^{H_{\max}} \left(\frac{\partial S}{\partial H} \right)_T dH. \quad (1)$$

From Maxwell's thermodynamic relation:

$$\left(\frac{\partial M}{\partial T} \right)_H = \left(\frac{\partial S}{\partial H} \right)_T \quad (2)$$

one can obtain the following expression:

$$|\Delta S_M| = \int_0^{H_{\max}} \left(\frac{\partial M}{\partial T} \right) dH \quad (3)$$

where H_{\max} is the maximum external field. According to the equation (3), the magnetic entropy change ($|\Delta S_M|$) depends on the temperature gradient of the magnetization and attains a maximum value around Curie temperature, at which the magnetization decays most rapidly.

In fact, the $|\Delta S_M|$ is often evaluated by some numerical approximation methods. One way of approximation is to directly use the measurements of the M - T curve under different field. In the case of small discrete field intervals, $|\Delta S_M|$ can be approximately from equation (3) as

$$|\Delta S_M| = \sum_i \left[\left(\frac{\partial M}{\partial T} \right)_{H_i} + \left(\frac{\partial M}{\partial T} \right)_{H_{i+1}} \right] \times \frac{\Delta H_i}{2} \quad (4)$$

where $(\partial M/\partial T)_{H_i}$ is the experimental value obtained from the M - T curve in field H_i . Another method is to use isothermal magnetization measurements at small discrete field and temperature intervals, $|\Delta S_M|$ can be approximately from equation (3) by

$$|\Delta S_M| = \sum_i \frac{M_i - M_{i+1}}{T_{i+1} - T_i} \Delta H_i. \quad (5)$$

In this article, we adopt the latter method to evaluate the magnetic entropy change associated with the magnetic field variation.

Figure 6 shows a part of the isothermal magnetization curves at different temperatures for sample $\text{La}_{2.5-x}\text{K}_{0.5+x}\text{Mn}_2\text{O}_{7+\delta}$ ($x = 0.25$). In our experiments, the changing rate of the magnetic field (20 Oe/s) is slow enough to get an isothermal M - T curve. The polycrystalline $\text{La}_{2.5-x}\text{K}_{0.5+x}\text{Mn}_2\text{O}_{7+\delta}$ samples exhibit considerably small magnetic hysteresis with coercivity of below 50 Oe. Figure 7 shows the temperature dependence of $|\Delta S_M|$ under different applied fields for $\text{La}_{2.5-x}\text{K}_{0.5+x}\text{Mn}_2\text{O}_{7+\delta}$. As expected from equation (3), the peaks of the magnetic entropy changes of the five samples are around each Curie temperature T_C . We found that the magnetic entropy change of $\text{La}_{2.5-x}\text{K}_{0.5+x}\text{Mn}_2\text{O}_{7+\delta}$ is comparable to that of $\text{La}_{1-x}\text{K}_x\text{MnO}_{3+\delta}$ [32]. The maximum $|\Delta S_M|$ is in the order of 1.4 J/kg.K for $\text{La}_{2.5-x}\text{K}_{0.5+x}\text{Mn}_2\text{O}_{7+\delta}$ with $x = 0.35$ upon 10 kOe applied field. However, due to the anisotropy exchange interaction existing in two-layered manganites, the T_C of

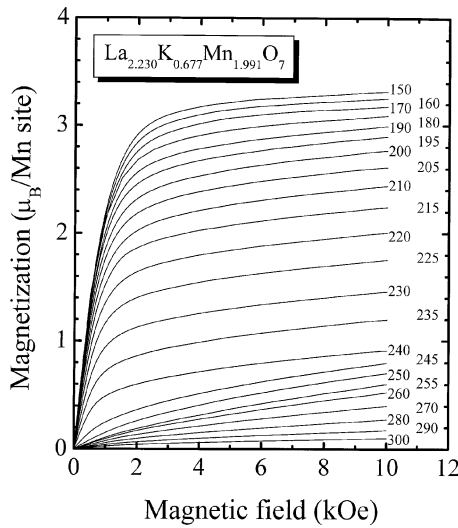


Fig. 6. Magnetization as function of applied field measured at different temperatures for polycrystalline $\text{La}_{2.5-x}\text{K}_{0.5+x}\text{Mn}_2\text{O}_{7+\delta}$ ($x = 0.25$). Only a part of isothermal magnetization data is presented.

$\text{La}_{2.5-x}\text{K}_{0.5+x}\text{Mn}_2\text{O}_{7+\delta}$ is reduced by 30 ~ 90 K as compared to that of $\text{La}_{1-x}\text{K}_x\text{MnO}_{3+\delta}$ and causes a shift in the peak of the $|\Delta S_M|$ to lower temperatures.

The experimental results indicate that although the electric properties and magnetoresistance effect of the two-layered $\text{La}_{2.5-x}\text{K}_{0.5+x}\text{Mn}_2\text{O}_{7+\delta}$ are quite different from those of the ABO_3 -type perovskites, their magnetocaloric properties are similar to those of latter materials. When a magnetic field is applied to this kind of material, the unpaired spins are aligned parallel to the field. Since the total entropy of spins plus the lattice remains constant, the entropy is removed from the spins system and goes into the lattice, which lowers the magnetic entropy and produces a net heat. On the contrary, when the field is removed from the magnetic sample, the spin tends to become random, which causes a net cooling. Therefore, the maximum of the magnetic entropy change always occurs around its magnetic ordering temperature. The results observed that the maximum of $|\Delta S_M|$ is restricted to a narrow temperature range around T_C (far above T_ρ) seem to indicate that the origin of the magnetic entropy change measured on $\text{La}_{2.5-x}\text{K}_{0.5+x}\text{Mn}_2\text{O}_{7+\delta}$ sample is mostly attributed to the intra-layer exchange interaction.

4 Conclusions

The use of sol-gel method enables the formation of polycrystalline layered-perovskites $\text{La}_{2.5-x}\text{K}_{0.5+x}\text{Mn}_2\text{O}_{7+\delta}$. Large deviation in T_ρ and T_C was found in these two-layered perovskite samples. Magnetoresistance effect was observed over a wide temperature range from low temperatures to the room temperature, and there is a systematic increase with decreasing temperatures in all samples. These behaviors are different from those of the well-known

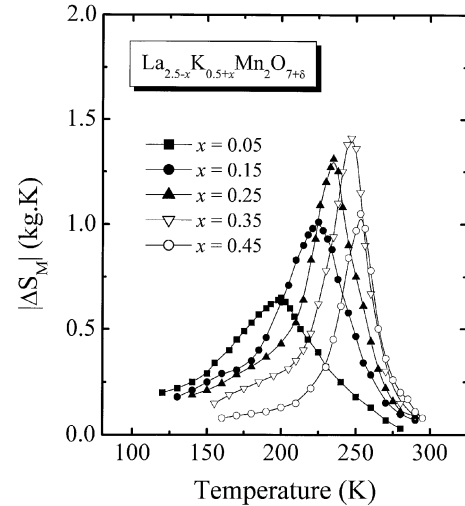


Fig. 7. Temperature dependence of magnetic entropy change upon an applied field $H_{\text{max}} = 10$ kOe for polycrystalline $\text{La}_{2.5-x}\text{K}_{0.5+x}\text{Mn}_2\text{O}_{7+\delta}$ perovskites.

ABO_3 -type perovskite manganites. The maximum of the magnetic entropy change for $\text{La}_{2.5-x}\text{K}_{0.5+x}\text{Mn}_2\text{O}_{7+\delta}$ peaks at its Curie temperature, and is comparable to that of $\text{La}_{1-x}\text{K}_x\text{MnO}_{3+\delta}$. Although the properties of our materials are far from optimal, further exploration if this layered manganites may prove fruitful.

This work is Supported by the National Natural Science Foundation of China under Grant No. 50072007, and the National Key Project for Basic Research (No. G1999064508), People's Republic of China.

References

1. R. Von Helmolt, J. Wecker, B. Holzapfel, L. Schultz, K. Samwer, Phys. Rev. Lett. **71**, 2331 (1993)
2. H.L. Ju, C. Kwon, Q. Li, R.L. Greene, T. Venkatesan, Appl. Phys. Lett. **65**, 2117 (1994)
3. H.L. Ju *et al.*, Phys. Rev. B **51**, 6143 (1995)
4. P. Schiffer, A.P. Ramirez, W. Bao, S.W. Cheong, Phys. Rev. Lett. **75**, 3336 (1995)
5. S. Jin *et al.*, Appl. Phys. Lett. **66**, 382 (1995)
6. H.Y. Hwang, S.W. Cheong, P.G. Radaelli, M. Marezio, B. Batlog, Phys. Rev. Lett. **75**, 914 (1996)
7. R. Mahendiran, S.K. Tiwari, A.K. Raychaurhuri, T.V. Ramakrishnan, R. Mahesh, N. Rangavittal, C.N.R. Rao, Phys. Rev. B **53**, 3348 (1996)
8. D.T. Morelli, A.M. Mance, J.V. Mantese, A.L. Micheli, J. Appl. Phys. **79**, 373 (1996).
9. Z.B. Guo, Y.W. Du, J.S. Zhu, H. Huang, W.P. Ding, D. Feng, Phys. Rev. Lett. **78**, 1142 (1997)
10. X.X. Zhang, J. Tejada, Y. Xin, G.F. Sun, K.W. Wong, X. Bohigas, Appl. Phys. Lett. **69**, 3596 (1996)
11. W. Zhong, W. Chen., W.P. Ding, N. Zhang, Y.W. Du, Q.J. Yan, Solid State Commun. **106**, 55 (1998)
12. W. Zhong *et al.*, Eur. Phys. J. B **3**, 169 (1998)

13. Y. Moritomo, Y. Tomioka, A. Asamitsu, Y. Tokura, Y. Matsui, *Nature* **380**, 141 (1996)
14. H. Asano, J. Hayakawa, M. Matsui, *Appl. Phys. Lett.* **68**, 3638 (1996)
15. H. Asano, J. Hayakawa, M. Matsui, *Jpn J. Appl. Phys. Lett.* **36**, L104 (1997)
16. T. Kimura, Y. Tomioka, H. Kuwahara, A. Asamitsu, M. Tamura, Y. Tokura, *Science* **274**, 1698 (1996)
17. R. Suryanarayanan, I. Zelenay, J. Berthon, *Mater. Res. Bull.* **32**, 595 (1997)
18. C.D. Potter, M. Swiatek, S.D. Bader, D.N. Argyiou, J.F. Mitchell, D.J. Miller, D.G. Hinks, J.D. Jorgensen, *Phys. Rev. B* **57**, 72 (1998)
19. D.N. Argyiou, J.F. Mitchell, C.D. Potter, S.D. Bader, R. Kleb, J.D. Jorgensen, *Phys. Rev. B* **55**, R11965 (1997)
20. D.N. Argyiou, J.F. Mitchell, J.B. Goodenough, O. Chmaissem, S. Short, J.D. Jorgensen, *Phys. Rev. Lett.* **78**, 1568 (1997)
21. J.F. Mitchell, D.N. Argyiou, J.D. Jorgensen, D.G. Hinks, C.D. Potter, S.D. Bader, *Phys. Rev. B* **55**, 63 (1997)
22. R. Mahesh, R. Wang, M. Itoh, *Phys. Rev. B* **57**, 104 (1998)
23. T.J. Zhou, Z. Yu, W. Zhong, X.N. Xu, H.H. Zhang, Y.W. Du, *J. Appl. Phys.* **85**, 7975 (1999).
24. C.D. Ling, J.E. Millburn, J.F. Mitchell, D.N. Argyiou, J. Linton, H.N. Bordallo, *Phys. Rev. B* **62**, 15096 (2000)
25. T. Kimura, A. Asamitsu, Y. Tomioka, Y. Tokura, *Phys. Rev. Lett.* **79**, 3720 (1997)
26. D.N. Argyiou, J.F. Mitchell, P.G. Radaelli, H.N. Bordallo, D.E. Cox, M. Medarde, J.D. Jorgensen, *Phys. Rev. B* **59**, 8695 (1999)
27. T. Kimura, R. Kumai, Y. Tokura, J.Q. Li, Y. Matsui, *Phys. Rev. B* **58**, 11081 (1998)
28. T. Hayashi, N. Miura, M. Tokunaga, T. Kimura, Y. Tokura, *J. Phys. Cond. Matt.* **10**, 11525 (1998)
29. R. Suryanarayanan, G. Dhallenne, A. Revcolevschi, W. Prellier, J.P. Renard, C. Dupas, W. Caliebe, T. Chatterji, *Solid State Commun.* **113**, 267 (2000)
30. M. Kubota, H. Fujioka, K. Ohoyama, K. Hirota, Y. Moritomo, H. Yoshizawa, Y. Endoh, *J. Phys. Chem. Solids* **60**, 116 (1999)
31. K. Hirota, Y. Moritomo, H. Fujioka, M. Kubota, H. Yoshizawa, Y. Endoh, *J. Phys. Soc. Jpn* **67**, 3380 (1998)
32. W. Zhong, W. Chen, W.P. Ding, N. Zhang, A. Hu, Y.W. Du, Q.J. Yan, *J. Magn. Magn. Mater.* **195**, 112 (1999)
33. N.W. Hurst, S.J. Gentry, A. Jones, B.D. McNicol, *Catal. Rev.* **24**, 233 (1982)
34. T. Nakamura, G. Petzow, L.J. Gauckler, *Matt. Res. Bull.* **14**, 649 (1979)
35. H. Asano, J. Hayakawa, M. Matsui, *Phys. Rev. B* **56**, 5395 (1997)
36. R. Mahesh, R. Mahendiran, A.K. Raychauhuri, C.N.R. Rao, *Appl. Phys. Lett.* **68**, 2291 (1996)
37. R. Mahendiran, R. Mahesh, A.K. Raychauhuri, C.N.R. Rao, *Solid State Commun.* **99**, 149 (1996)